Formation of a Stable Decagonal Quasicrystalline Al-Pd-Mn Surface Layer

D. Naumović,[1] P. Aebi,[1] L. Schlapbach,[1] C. Beeli,[2] K. Kunze,[3] T. A. Lograsso,[4] and D. W. Delaney[4]

[1]*Institut de Physique, Université de Fribourg, Pérolles, CH-1700 Fribourg, Switzerland*
[2]*Laboratory of Solid State Physics, ETHZ, CH-8093 Zürich, Switzerland*
[3]*Institute of Geology, ETHZ, CH-8092 Zürich, Switzerland*
[4]*Ames Laboratory, Iowa State University, Ames, Iowa 50011*
(Received 18 July 2001; published 19 October 2001)

We report the *in situ* formation of an ordered equilibrium decagonal Al-Pd-Mn quasicrystal overlayer on the fivefold symmetric surface of an icosahedral Al-Pd-Mn monograin. The decagonal structure of the epilayer is evidenced by x-ray photoelectron diffraction, low-energy electron diffraction, and electron backscatter diffraction. This overlayer is also characterized by a reduced density of states near the Fermi edge as expected for quasicrystals. This is the first time that a millimeter-size surface of the stable decagonal Al-Pd-Mn is obtained, studied, and compared to its icosahedral counterpart.

Quasicrystals (QCs) are exceptional in many aspects. They emerged from the rather complex Al-Mn phase diagram at the beginning of the 1980's [1]. Their structure is infringing upon the classic rules of crystallography: They are nonperiodic, but long-range ordered, and they include forbidden symmetry axes such as fivefold ($5f$), $8f$, $10f$, or $12f$, depending on the alloy [2]. Furthermore, the electronic structure of QCs is quite unexpected. The electrical resistivity is 1000 times higher than their constituents, metals, and inversely proportional to temperature [3]. Despite the lack of periodicity, a bandlike behavior is observed in the electronic structure [4,5]. QCs also exhibit properties which are directly attractive for applications, such as low friction, low adhesion, or increased hardness [6].

Even today, producing QCs, and especially monograin samples of stable phases, remains a challenge. In that sense, one of the most fruitful systems is Al-Pd-Mn. In 1990, Tsai *et al.* discovered a first stable icosahedral (i) QC (i-$Al_{70}Pd_{20}Mn_{10}$) in the ternary Al-Pd-Mn system [7]. It is possible to produce high-quality large monograins of this alloy. This facilitates experiments, such as neutron or x-ray diffraction, or surface experiments. A *stable*, *decagonal* (d) Al-Pd-Mn QC was found by Beeli, Nissen, and Robadey [8]. It exists only in a very narrow area in the phase diagram [9]. Therefore, it is difficult to obtain a single-phase specimen with high quality of the decagonal structure. Interestingly, a decagonal QC with high structural quality can be obtained by annealing rapidly quenched tapes of an $Al_{69.8}Pd_{12.1}Mn_{18.1}$ alloy, which contains a metastable i-phase, but has the equilibrium composition of the d-phase [8]. Thus, the icosahedral long-range order is coherently transformed into decagonal long-range order. Furthermore, single-grain samples can be produced only by nonequilibrium processes via metastable reactions, and, generally, only by chance single grains with diameters of 0.1 mm are produced. Nevertheless, Al-Pd-Mn has the only known phase diagram containing two stable QC phases, the i- and d-phase.

Until now, many surface experiments have been reported on monograin i-Al-Pd-Mn. Clean surfaces are prepared either by fracturing [10–12] or by ion sputtering, and by annealing. Composition changes are induced by preferential sputtering of the lightest elements, or by thermal diffusion. For annealings <400 °C subsequent or simultaneous to sputtering, a crystalline phase with cubic domains ($Al_{55}Pd_{40}Mn_5$) [13–18] or a *metastable* decagonal quasicrystalline ($Al_{22}Pd_{56}Mn_{22}$) phase [19] was observed, respectively. Further annealing of these surfaces at ~450 to 650 °C restores a bulk-terminated icosahedral surface and a bulklike composition. Such surfaces are characterized by a reduced density of states close to the Fermi level (E_F), in contrast to usual metallic surfaces [4,12,16,17,20]. Annealing sputtered surfaces at higher temperatures produces either Pd or Mn enrichment (possibly depending on the initial bulk composition), which leads to a surface phase selection according to the local equilibrium controlled by the phase diagram. An irreversible precipitation of secondary phases is even reported [21]. The Pd-rich surfaces $Al_{>66}Pd_{32}Mn_{<2}$ [14,22] or $Al_{50}Pd_{49}Mn_1$ [18] were interpreted as cubic with domains and the Mn-rich $Al_{75}Pd_6Mn_{19}$ surface [23] as crystalline orthorhombic Al_3Mn. The reported crystalline phases are epitaxially grown on the substrate and rather ordered.

In this work, we produce for the first time a large surface of the *stable* decagonal quasicrystalline d-Al-Pd-Mn. The $10f$ surface of d-Al-Pd-Mn is epitaxially grown as a single-domain overlayer on the $5f$ i-Al-Pd-Mn, with the $10f$ axis of the overlayer parallel to the $5f$ axis of the substrate. The Mn-rich decagonal overlayer is produced *in situ* by sputtering and annealing the $5f$ i-Al-Pd-Mn at ~650 °C. The results on geometrical (Fig. 1) and electronic structure (Fig. 2), obtained with low-energy electron diffraction (LEED), x-ray photoelectron diffraction (XPD), electron backscatter diffraction (EBSD), and ultraviolet photoemission (UPS), clearly demonstrate that both the icosahedral surface and the decagonal epilayer can be identified with the corresponding stable bulk phases.
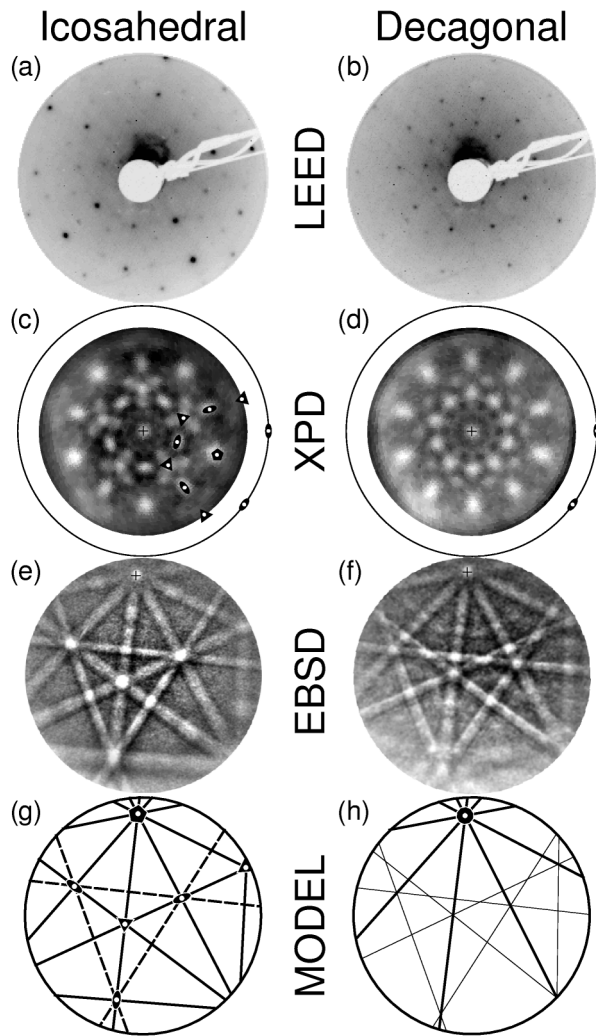

Icosahedral

Decagonal

(a)

(b)

LEED

(c)

(d)

XPD

(e)

(f)

EBSD

(g)

(h)

MODEL

FIG. 1. LEED patterns taken at 60 eV (high intensity in black) from a monograin i-Al-Pd-Mn cut perpendicularly to a $5f$-symmetry axis: (a) the bulk-terminated icosahedral quasicrystalline i-Al$_{68}$Pd$_{26}$Mn$_6$ surface obtained after sputtering and annealing at 550 °C; (b) the stable decagonal quasicrystalline d-Al$_{76}$Pd$_{11}$Mn$_{13}$ overlayer obtained after sputtering and annealing at 650 °C. XPD patterns of Pd $3d_{5/2}$ ($E_{kin} = 915$ eV, high intensity in white) with indicated normal emission (+), grazing emission (outer circle), $2f$-(ellipse), $3f$-(triangle), $5f$-(pentagon)symmetry axes, taken from (c), the icosahedral surface described in (a); (d) the decagonal surface described in (b). EBSD patterns [high intensity in white; sample normal (+)] taken from (e), the icosahedral surface described in (a); (f) the decagonal surface described in (b). Projections generated by a pattern recognition procedure, with indicated $2f$-, $3f$-, $5f$-(as above), $10f$-(decagon)symmetry axes, and $2f$-(solid thick line), $5f$-(dashed thick line)symmetry planes; (g) identifying (e) as quasicrystalline icosahedral; (h) identifying (f) as quasicrystalline decagonal, with additional first order rhombohedral planes (thin solid lines).

The photoemission experiments were performed in a VG ESCALAB Mk II spectrometer with a base pressure in the 10^{-11} mbar range. The sample stage is modified for motorized sequential angle-scanning data acquisition over the full solid angle [24]. Mg K_α radiation ($h\nu = 1253.6$ eV) was used for x-ray photoelectron
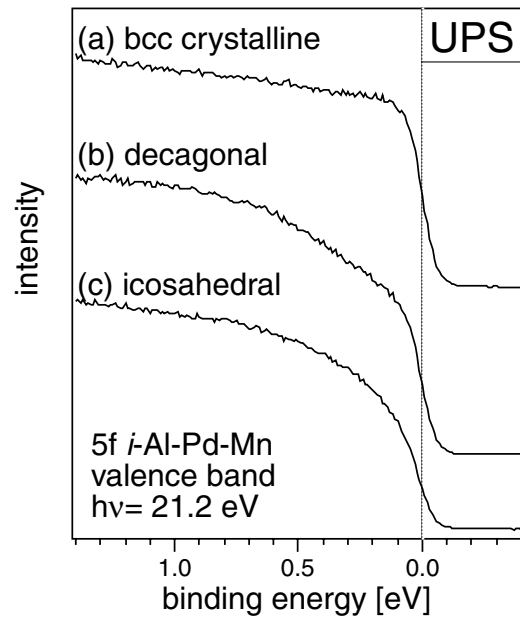
(a) bcc crystalline   UPS

intensity

(b) decagonal

(c) icosahedral

5f i-Al-Pd-Mn
valence band
hν= 21.2 eV

1.0   0.5   0.0
binding energy [eV]

FIG. 2. Room-temperature valence-band spectra displaying the near E_F region, taken with monochromatized He-I radiation ($h\nu = 21.2$ eV; analyzer energy resolution: 30 meV), (a) of the crystalline surface with bcc domains (Al$_{53}$Pd$_{41}$Mn$_6$; sputtered), (b) of the Mn-rich stable decagonal quasicrystalline overlayer (Al$_{76}$Pd$_{11}$Mn$_{13}$, sputtered and annealed at 650 °C), and (c) of the bulk-terminated icosahedral quasicrystalline surface (Al$_{68}$Pd$_{26}$Mn$_6$, sputtered and annealed at 550 °C).

spectroscopy (XPS) in order to check the cleanliness and to determine the composition [25] within the probing depth (mean free path of photoelectrons $\sim$20 Å). XPD served to study the geometrical structure of the surface [26]. In angle-scanned XPD, the intensity variations of photoemitted core-level electrons are recorded as a function of emission angle and stereographically projected in a grey scaled map. For kinetic energies >500 eV, photoelectrons leaving the emitter atom are strongly focused in the forward direction by neighboring atom potentials [26]. So, the intensity is enhanced along densely packed atomic rows or planes. Thus, XPD evidences the average local order around a selected chemical species. UPS was performed with monochromatized He-Iα radiation (21.2 eV) [27], and with the analyzer energy resolution set to 30 meV. All measurements are performed at room temperature.

The symmetry and orientation of substrate and layer were verified *ex situ* by EBSD [28]. EBSD patterns were recorded using a standard SEM CamScan CS44LB, equipped with a 50 mm diameter area detector (scintillator and camera) placed parallel to the incident beam. Diffraction patterns are formed from the spatial intensity distribution of backscattered electrons, which are induced by a focused stationary electron beam (15 kV, 3 nA). The sample surface is tilted 70° against the beam towards the detector. The spatial resolution is in the range of some tenths of a micrometer and anisotropic due to the 70° tilt. Bands of higher intensity arise between pairs of pseudo-Kikuchi lines, the center of which marks the

projection of diffracting symmetry planes onto the detector screen. These bands are detected in digitized EBSD patterns by image processing using a Hough transform [29]. The software OIM2.0 (TSL Inc.) was modified by us incorporating quasicrystallography, so that the model pattern could be recalculated which fits best with the detected diffraction bands for EBSD patterns of any orientation and symmetry.

The i-$Al_{71.6}Pd_{19.6}Mn_{8.6}$ quasicrystal ingot was grown using the Bridgman method [30]. The sample was an 1.3 mm thick disk with a diameter of 8 mm. It was oriented perpendicular to a $5f$-symmetry axis within $0.25°$ and polished with diamond paste and colloidal silica. It was cleaned *in situ* by room-temperature Ar^+ sputtering at 1 and 0.75 keV during 15 to 60 min (sample current: 1.0–1.5 $\mu A/cm^2$; estimated sputter rate: 1–2 Å/min) followed by annealing at indicated surface temperatures (pyrometer controlled) between 550 and 700 °C during 5 min (an additional 10–20 min was necessary to reach the desired value).

For the preparation of the icosahedral surface, sputtering and subsequent annealing to 550 °C resulted in XPS compositions of $Al_{53}Pd_{41}Mn_6$ and $Al_{68}Pd_{26}Mn_6$, respectively. However, for annealings at 650 °C (typically three sputter/anneal cycles are necessary to achieve a clean and pure d-phase layer), the surface becomes decagonal with a modified composition of $Al_{76}Pd_{11}Mn_{13}$. Such a composition is compatible with the *stable* decagonal QC composition ($Al_{69.8}Pd_{12.1}Mn_{18.1}$) [8]. In addition, the decagonal overlayer, once created, remains stable up to 700 °C (the highest probed temperature), and possibly beyond, as no sign of the occurrence of another phase is observed. This is in contrast to the composition of a *metastable* decagonal $Al_{22}Pd_{56}Mn_{22}$ phase, which differs vastly from the known bulk decagonal phase and where an icosahedral surface is recovered after annealing >400 °C [19]. After 15 to 30 min sputtering the decagonal surface, the composition is $Al_{66}Pd_{15}Mn_{19}$ and a 5 min annealing at 650 °C is sufficient to recover the decagonal surface. In contrast, typically 5 h of sputtering interrupted by several subsequent annealings at 550 °C are necessary to recover the icosahedral surface. Therefore, transformation from the decagonal back to the icosahedral surface is also possible.

Figure 1 displays the experimental data comparing the geometrical structure of the icosahedral bulk-terminated surface, and of the stable decagonal overlayer, measured with LEED, XPD, and EBSD. The icosahedral surface is characterized by a $5f$ LEED pattern [Fig. 1(a)], while the LEED picture of the decagonal overlayer [Fig. 1(b)] is $10f$ symmetric. This latter displays four rings of ten fine spots. The relationship between the radii of these four rings is proportional to the golden mean τ, confirming a quasicrystalline ordering of the overlayer. LEED spots are visible over a wide range of energies (12–140 eV). This indicates the long-range lateral ordering of the overlayer $10f$ surface, compatible with a stable decagonal quasicrystalline phase. Note that this pattern drastically differs from

the ones taken from the pseudo-$10f$ surfaces with crystalline domains [13,14,18,22]. Decagonal LEED patterns have been obtained from d-Al-Ni-Co [31].

The Pd $3d_{5/2}$ XPD pattern of the bulk-terminated $5f$ surface is shown in Fig. 1(c). The main high-intensity spots can be easily identified with the $2f$-, $3f$-, and $5f$-symmetry axes of the icosahedral group projected stereographically [14,17,32,22], with a $5f$-symmetry axis in the center (normal emission). These experimental patterns can be reproduced by single-scattering cluster calculations using clusters as inferred from structural models of the i-Al-Pd-Mn phase, confirming that the near surface region is quasicrystalline [32]. So we conclude that the average local environment around the Pd emitter atoms is icosahedral (idem for Al and Mn, not shown [32]). In contrast, Fig. 1(d) displays the XPD pattern of the Mn-rich stable decagonal overlayer, with an evident overall $10f$ symmetry and a central $10f$-symmetry axis. Here, three rings of equivalent intense spots replace the alternation of spots identified as $2f$-, $3f$-, and $5f$-symmetry axes in Fig. 1(c). This clearly indicates an average short-range decagonal ordering of the overlayer. Strong epitaxial relationships exist between the icosahedral bulk and the decagonal overlayer. The decagonal XPD pattern resembles the XPD [33] and secondary electron imaging (SEI) [34] patterns taken from d-Al-Ni-Co. Note that the SEI pattern of the decagonal metastable $Al_{22}Pd_{56}Mn_{22}$ overlayer resembles the sputtered d-Al-Ni-Co surface [19]. The XPD patterns of the Pd-rich pseudo-$10f$ surface [14,22] and of the sputtered d-Al-Ni-Co surface [33] were both interpreted as crystalline with bcc domains.

Figures 1(e) and 1(f) show the EBSD results obtained *ex situ* from the icosahedral and decagonal phase created on the $5f$ i-Al-Pd-Mn sample. The EBSD pattern presented in Fig. 1(e) is identified as corresponding to the i-phase [Fig. 1(g)] with a $5f$ axis coinciding with the sample normal (marked by $+$). Further $2f$- and $3f$ axes are situated at crossings of $2f$- and $5f$-symmetric planes as indicated in Fig. 1(g). These latter symmetry axes, as well as $5f$-symmetric planes, do not exist in the pattern [Fig. 1(f)] identified as decagonal [Fig. 1(h)]. Here, a $10f$ axis coincides with the sample normal, and only the radial $2f$-symmetric Kikuchi bands crossing the $10f$ axis persist. As EBSD arises from 200 to 500 Å depth, the thickness of the stable d-phase is at least of that order of magnitude (consistent with the thickness deduced from the sputter rate and the needed time to remove the layer). Once the decagonal overlayer formed, the appearance of the icosahedral pattern (alone or superimposed to the decagonal pattern with lower contrast) indicates that some patches ($<1\%$) of the surface are covered with a thinner decagonal overlayer or remain uncovered. In addition, this evidences the strong structural and orientational relationship between the icosahedral bulk and the decagonal overlayer.

Figure 2 displays valence-band spectra taken at room temperature of the icosahedral bulk-terminated surface, of the stable decagonal overlayer, and of a crystalline phase,

obtained by sputtering the icosahedral surface. This latter $5f$ surface consists of five bcc (113) domains rotated by 72° with respect to each other as seen with XPD [17]. The density of states remains high and linear over the complete range of energy and the Fermi edge is sharp, as expected from a metal [Fig. 2(a)]. In Fig. 2(c), the icosahedral surface exhibits a completely different behavior. A distinct decrease of the density of states near E_F, interpreted as the opening of a pseudogap, is observed, as expected from a QC [4,16–17,20,35]. Finally, the density of states of the stable decagonal overlayer [Fig. 2(b)] is lowered close to E_F, as for the icosahedral quasicrystalline surface. However, the shape of the curve is slightly different, with a steeper Fermi cutoff. This is probably related to the fact that the decagonal surface is periodic in one dimension (along the surface normal) and that the quantity of Mn (Mn $3d$ states determine the spectral weight close to E_F [35]) is doubled in the decagonal phase compared to the icosahedral and crystalline bcc phases.

An important point to be discussed is how to ensure the quasicrystallinity of the surface. In previous work on i-Al-Pd-Mn [16,17], we demonstrated that a combination of geometrical and electronic structure techniques can efficiently characterize the QC surfaces. First, the ordering and the symmetry within differently prepared surfaces were probed with XPD and LEED. But note that a $5f$- [17] or $10f$-symmetry [14,22] can also be due to a combination of domains and not only to the intrinsic QC symmetry. Second, a distinct suppression of spectral weight of the density of states close to E_F was observed on quasicrystalline terminated surfaces by UPS. Here, one has to be aware that a suppressed density of states is also reported on a crystalline approximant of QC [12]. Whereas, even a slight disordering of the QC surface, induced by a one-minute ion sputtering, produces a sharp Fermi edge cutoff, characteristic of a metallic surface, with no apparent composition changes [20]. So, a careful evaluation of the geometrical and electronic structure data, together with the composition, is essential to identify quasicrystallinity or, at least, to exclude crystallinity of the surface.

In summary, this work presents for the first time the formation of an extended and ordered stable decagonal quasicrystalline overlayer on $5f$ i-Al-Pd-Mn by sputtering and annealing at 650 °C. This overlayer was characterized, at different scales, with three structure techniques: XPD, LEED, and EBSD. We clearly identified the icosahedral and decagonal symmetries of the surfaces and evidenced the epitaxial relationships between the decagonal overlayer and the icosahedral bulk. Furthermore the decagonal overlayer exhibited a suppressed density of states near E_F as seen with UPS, as expected for quasicrystals. The production of the two quasicrystalline, decagonal and icosahedral, alloys of the same elemental Al-Pd-Mn family gives the unique opportunity to study and compare the properties of these two phases.

[1] D. Shechtman et al., Phys. Rev. Lett. **53**, 1951 (1984).
[2] C. Janot, *Quasicrystals: A Primer* (Oxford University Press, Oxford, 1994), 2nd ed.
[3] S. J. Poon, Adv. Phys. **41**, 303 (1992).
[4] X. Wu et al., Phys. Rev. Lett. **75**, 4540 (1995).
[5] E. Rotenberg et al., Nature (London) **406**, 602 (2000).
[6] J.-M. Dubois, Phys. Scr. **T49**, 17 (1993).
[7] A. P. Tsai et al., Philos. Mag. Lett. **61**, 9 (1990).
[8] C. Beeli, H.-U. Nissen, and J. Robadey, Philos. Mag. Lett. **63**, 87 (1991); C. Beeli et al., in *Proceedings of the 5th International Conference on Quasicrystals, Avignon, 1994,* edited by C. Janot and R. Mosseri (World Scientific, Singapore, 1995), p. 680.
[9] T. Gödecke and R. Lück, Z. Metallkd. **86**, 109 (1995).
[10] Ph. Ebert et al., Phys. Rev. Lett. **77**, 3827 (1996); Phys. Rev. B **57**, 2821 (1998); ibid. **60**, 874 (1999).
[11] G. Neuhold et al., Phys. Rev. B **58**, 734 (1998).
[12] V. Fournée et al., Phys. Rev. B **62**, 14 049 (2000).
[13] Z. Shen et al., Phys. Rev. Lett. **78**, 1050 (1997); Phys. Rev. B **58**, 9961 (1998); Surf. Sci. **450**, 1 (2000).
[14] D. Naumović et al., in *Proceedings of the 6th International Conference on Quasicrystals, Tokyo, 1997,* edited by S. Takeuchi and T. Fujiwara (World Scientific, Singapore, 1998), p. 749.
[15] B. Bolliger et al., Phys. Rev. Lett. **80**, 5369 (1998).
[16] D. Naumović et al., Phys. Rev. B **60**, R16 330 (1999).
[17] D. Naumović et al., Mater. Sci. Eng. A **294–296**, 882 (2000).
[18] F. Schmithüsen et al., Surf. Sci. **444**, 113 (2000).
[19] B. Bolliger et al., Phys. Rev. Lett. **82**, 763 (1999).
[20] T. Schaub et al., Eur. Phys. J. B **20**, 183 (2001).
[21] P. A. Thiel et al., in *Physical Properties of Quasicrystals,* edited by Z. M. Stadnik (Springer-Verlag, Berlin, 1999), p. 327.
[22] D. Naumović et al., Surf. Sci. **433–435**, 302 (1999).
[23] J. Ledieu et al., Mater. Sci. Eng. A **294–296**, 871 (2000).
[24] J. Osterwalder et al., Phys. Rev. B **44**, 13 764 (1991).
[25] Note that XPS concentrations cannot directly be compared with a true stoichiometry because it is based only on intensity ratios including core-level cross sections; see [14,22].
[26] See, e.g., C. S. Fadley, Surf. Sci. Rep. **19**, 231 (1993).
[27] Th. Pillo et al., J. Electron. Spectrosc. Relat. Phenom. **97**, 243 (1998).
[28] J. A. Venables and C. J. Harland, Philos. Mag. **27**, 1193 (1973).
[29] B. L. Adams, S. I. Wright, and K. Kunze, Metall. Trans. A **24**, 819 (1993); K. Kunze et al., Textures Microstruct. **20**, 41 (1993).
[30] D. W. Delaney, T. E. Bloomer, and T. A. Lograsso, in *New Horizons in Quasicrystals,* edited by A. I. Goldman et al. (World Scientific, Singapore, 1997), p. 45.
[31] M. Gierer et al., Surf. Sci. **463**, L654 (2000).
[32] D. Naumović et al., in *New Horizons in Quasicrystals,* (Ref. [30]), p. 86.
[33] M. Shimoda et al., Surf. Sci. **454–456**, 11 (2000).
[34] M. Zurkirch et al., Phys. Rev. B **58**, 14 113 (1998).
[35] Z. M. Stadnik et al., Phys. Rev. Lett. **77**, 1777 (1996).